Journal of Hydrology 428–429 (2012) 170–181

Contents lists available at SciVerse ScienceDirect

Journal of Hydrology

journal homepage: www.elsevier.com/locate/jhydrol

Forests and erosion: Insights from a study of suspended-sediment dynamics in an overland flow-prone rainforest catchment

Alexander Zimmermann [a,*], Till Francke [a], Helmut Elsenbeer [a,b]

[a] Institute of Earth and Environmental Sciences, University of Potsdam, Karl-Liebknecht-Str. 24-25, 14476 Potsdam, Germany
[b] Smithsonian Tropical Research Institute, Apartado 0843-03092, Balboa, Ancón, Panama

ARTICLE INFO

Article history:
Received 27 October 2010
Received in revised form 14 November 2011
Accepted 30 January 2012
Available online 9 February 2012
This manuscript was handled by Konstantine P. Georgakakos, Editor-in-Chief, with the assistance of Michael Bruen, Associate Editor

Keywords:
Rainforest
Overland flow
Erosion
Suspended-sediment yield
Quantile Regression Forest model
Panama Canal watershed

SUMMARY

Forests seem to represent low-erosion systems, according to most, but not all, studies of suspended-sediment yield. We surmised that this impression reflects an accidental bias in the selection of monitoring sites towards those with prevailing vertical hydrological flowpaths, rather than a tight causal link between vegetation cover and erosion alone. To evaluate this conjecture, we monitored, over a 2-year period, a 3.3 ha old-growth rainforest catchment prone to frequent and widespread overland flow. We sampled stream flow at two and overland flow at three sites in a nested arrangement on a within-event basis, and monitored the spatial and temporal frequency of overland flow. Suspended-sediment concentrations were modeled with Random Forest and Quantile Regression Forest to be able to estimate the annual yields for the 2 years, which amounted to 1 t ha^{-1} and 2 t ha^{-1} in a year with below-average and with average precipitation, respectively. These estimates place our monitoring site near the high end of reported suspended-sediment yields and lend credence to the notion that low yields reflect primarily the dominance of vertical flowpaths and not necessarily and exclusively the kind of vegetative cover. Undisturbed forest and surface erosion are certainly no contradiction in terms even in the absence of mass movements.

1. Introduction

Vegetation controls erosion in many ways and it is generally assumed that forest cover is an effective control (e.g. Lal, 1983; Rey, 2003; Bruijnzeel, 2004; Sidle et al., 2006; Garzía-Ruiz et al., 2008; Stickler et al., 2009; Verbist et al., 2010). Currently, most literature on suspended-sediment dynamics in forest ecosystems supports this assumption (Fritsch and Sarrailh, 1986; Baharuddin, 1988; Grayson et al., 1993; Malmer, 1996; Stott et al., 2001; Swank et al., 2001; Gökbulak et al., 2008), and estimates of sediment export from undisturbed forested catchments serve as benchmarks for the assessment of erosion processes under different land uses (Fritsch and Sarrailh, 1986; Sidle et al., 2006) and forest practices (Baharuddin, 1988; Grayson et al., 1993; Malmer, 1996; Stott et al., 2001; Swank et al., 2001). The results from a few studies (Douglas et al., 1992; Sayer et al., 2004, 2006b; Ide et al., 2009), however, are not in line with the widespread belief that undisturbed forests represent low erosion systems.

In order to better understand the apparent heterogeneity of suspended-sediment yields from forest ecosystems we conducted a literature survey that excluded effects of scale (cf. Fig. 6, Verbist et al., 2010), rainfall (cf. Fig. 10a, Ide et al., 2009), former disturbance (cf. Fig. 6, Clark and Walsh, 2006), and processes that override suspended-sediment dynamics (e.g. large-scale mass wasting processes (cf. Fig. 10, Bruijnzeel, 2004)). Hence, we only considered studies that fulfilled the following conditions: (1) catchment size of up to approximately 100 ha only, (2) mean annual precipitation >1000 mm, (3) undisturbed, and (4) no mass wasting. Given that these constraints did not reduce the spread in sediment yields, we scrutinized these studies with regards to prevailing hydrological flowpaths, i.e., vertical vs. near-surface lateral (overland flow, pipe flow, and return flow) according to the scheme proposed earlier (Elsenbeer, 2001). Given this framework, two issues became apparent.

First, although the majority of studies that estimated suspended-sediment yields provided only limited information on prevailing flowpaths, the few available data lead us to assume that the largest sediment exports occur at sites with frequent near-surface flow (evidence from Danum Valley, Malaysia (Sayer et al., 2004, 2006b; Clark and Walsh, 2006); observations at a Japanese site (Ide et al., 2009)). In contrast, such flowpaths are believed to be absent or restricted to riparian zones at sites with very low sediment yields (Grayson et al., 1993; Malmer, 1996; Swank et al., 2001).

Second, sediment data from undisturbed forests with prevailing lateral flowpaths are sparse (Fig. 1), and one could argue that the

* Corresponding author. Tel.: +49 331 977 2047; fax: +49 331 977 2068.
E-mail address: alexander.zimmermann.ii@uni-potsdam.de (A. Zimmermann).

0022-1694/$ - see front matter © 2012 Elsevier B.V. All rights reserved.
doi:10.1016/j.jhydrol.2012.01.039

few studied sites do not provide enough evidence to modify the prevailing knowledge concerning erosion processes in forests. We believe, however, that the available suspended-sediment data give a biased impression due to the over-representation of vertical flowpath-dominated sampling sites (Fig. 1). A closer look at the hydrological literature reveals that forested areas with a prevailing lateral flow component at the soil surface are not the exception; instead, these sites are numerous (evidence from Central America (Rouse et al., 1986; Godsey et al., 2004; Schellekens et al., 2004; Loos and Elsenbeer, 2011), South America (Elsenbeer and Vertessy, 2000; Johnson et al., 2006; de Moraes et al., 2006), Europe (Badoux et al., 2006), Africa (Wierda et al., 1989), Asia (Chatterjea, 1989; Sayer et al., 2004, 2006b; Clark and Walsh, 2006; Ide et al., 2008; Gomi et al., 2008), and Australia (Bonell and Gilmour, 1978)).

This literature survey suggests a link between suspended-sediment yield of forest catchments and the mode of runoff generation: Areas with prevailing vertical flowpaths produce little sediment, whereas lateral, near-surface flowpath-dominated catchments deliver more despite their forest cover. In other words, although there is no doubt that undisturbed forests have lower erosion rates than their disturbed counterparts (Fritsch and Sarrailh, 1986; Douglas et al., 1992; Malmer, 1996; Chappell et al., 1999; Bruijnzeel, 2004; Sidle et al., 2006), we argue that under certain hydrological conditions forests are not capable of preventing erosion completely. To check if there is any truth to this conjecture, we monitored overland flow and streamflow suspended-sediment concentrations in a small, undisturbed forest catchment prone to frequent and widespread overland flow and modeled suspended-sediment concentrations in order to calculate event-based and annual yields. Since estimates of sediment yields are usually associated with large uncertainties, we applied methods that enabled us to assess the accuracy and precision of our predictions.

2. Methods

2.1. General description of the study site

The study site, Lutzito catchment (LC), is a 3.3 ha catchment located on Barro Colorado Island, Panama (9°9′32″N, 79°50′17″W; Fig. 2). The island was isolated from the main land in 1914 after damming the Chagres River to form Lake Gatun, which is part of the Panama Canal. The topography of LC is heterogeneous: gullies and rills dissect slopes that reach 35° in places. Slope lengths range from 20 to 100 m. In spite of steep terrain and frequent large amounts of rainfall, mass movements are very rare: Dietrich et al. (1982) referred to one landslide in 1959.

The vegetation of Barro Colorado is classified as tropical semi-deciduous moist forest (Foster and Brokaw, 1982). The forest in LC (Fig. 2d) is secondary growth of more than 100 years of age (Kenoyer, 1929). The vegetation has not been disturbed since the island was declared a reserve in 1923 (Foster and Brokaw, 1982). Stand height is 25–35 m with few emergents approaching 45 m. A vegetation survey at the study site, considering trees greater than 5 cm diameter at breast height, revealed that a single hectare contains approximately 98 tree species and 1140 tree stems, which form a basal area of 35 m^2 ha^{-1} (Zimmermann et al., 2009).

The climate features distinct wet and dry seasons (Fig. 3a). The wet season lasts approximately from May to mid-December. Total annual rainfall averages 2623 ± 458 mm (mean ± 1 sd, n = 81, data from 1929 to 2009, Smithsonian Tropical Research Institute, Environmental Science Program). Rainfall distribution during the wet season is fairly uniform, except for a maximum of more than 400 mm in November (Fig. 3a). LC is underlain by tuffaceous siltstone of the Caimito Marine Facies (Woodring, 1958). Soils are classified as Ferric Cambisols (Baillie et al., 2007) and reach depths between 0.3 m on some ridges and steep slopes and 1 m elsewhere.

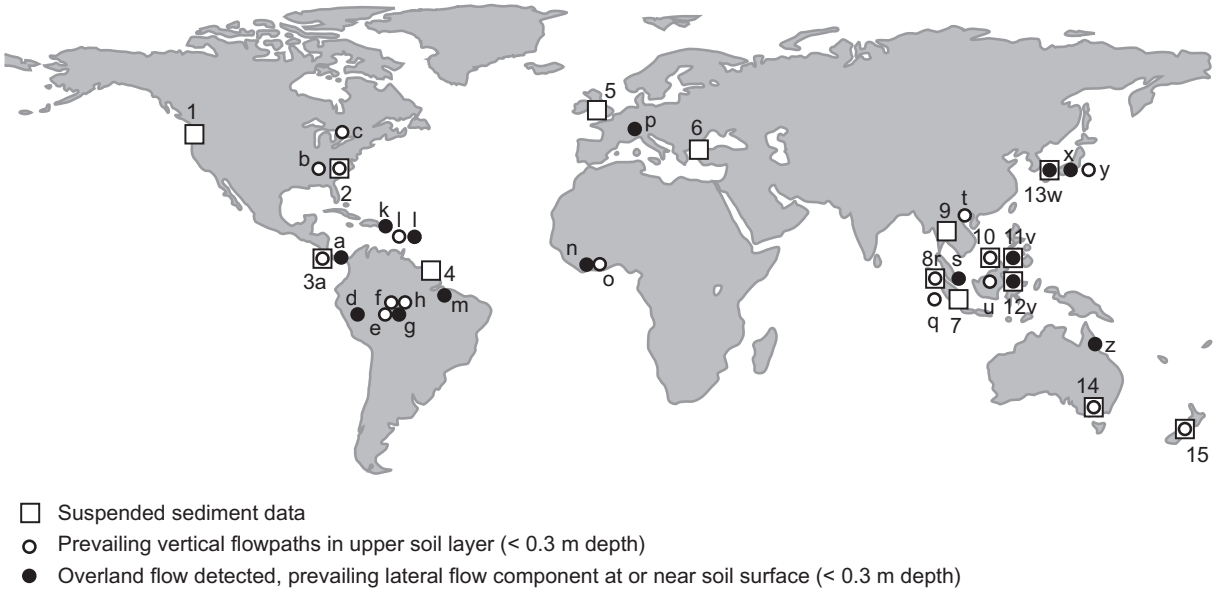

Fig. 1. A global overview of studies providing annual suspended-sediment yields from undisturbed forest catchments (boxes) and of studies that investigated flowpaths in this environment (circles). Empty boxes denote study sites where no information on prevailing flowpaths is available. The numbers refer to sediment studies, whereas letters refer to studies that investigated flowpaths; in case a sediment study provided also information on prevailing flowpaths only a number is given (1 – Brown and Krygier (1971) and Beschta (1978); 2 – Swank et al. (2001); 3 – Leigh (1999); 4 – Fritsch and Sarrailh (1986); 5 – Stott et al. (2001); 6 – Gökbulak et al. (2008); 7 – Baharuddin and Abduhl Rahim (1994); 8 – Baharuddin (1988); 9 – Douglas (1999); 10 – Malmer (1996); 11 – Douglas et al. (1992); 12 – Sayer et al. (2006b); 13 – Ide et al. (2009); 14 – Grayson et al. (1993); 15 – O'Loughlin et al. (1978); a – Godsey et al. (2004); b – Tromp-van Meerveld and McDonnell (2006); c – Peters et al. (1995); d – Elsenbeer and Vertessy (2000); e – Germer et al. (2010); f – Lesack (1993); g – Johnson et al. (2006); h – Nortcliff and Thornes (1984); k – Schellekens et al. (2004); l – Rouse et al. (1986); m – de Moraes et al. (2006); n – Wierda et al. (1989); o – Roose (1979); p – Badoux et al. (2006); q – Nogushi et al. (1997); r – Chappell et al. (2005); s – Chatterjea (1989); t – Ziegler et al. (2004); u – Dykes and Thornes (2000); v – Sinun et al. (1992), Sayer et al. (2004, 2006b), and Clark and Walsh (2006); w – Ide et al. (2008); x – Gomi et al. (2008); y – Sidle et al. (2000); z – Bonell and Gilmour (1978)). The selection of sites is restricted to several boundary conditions mentioned in Section 1.

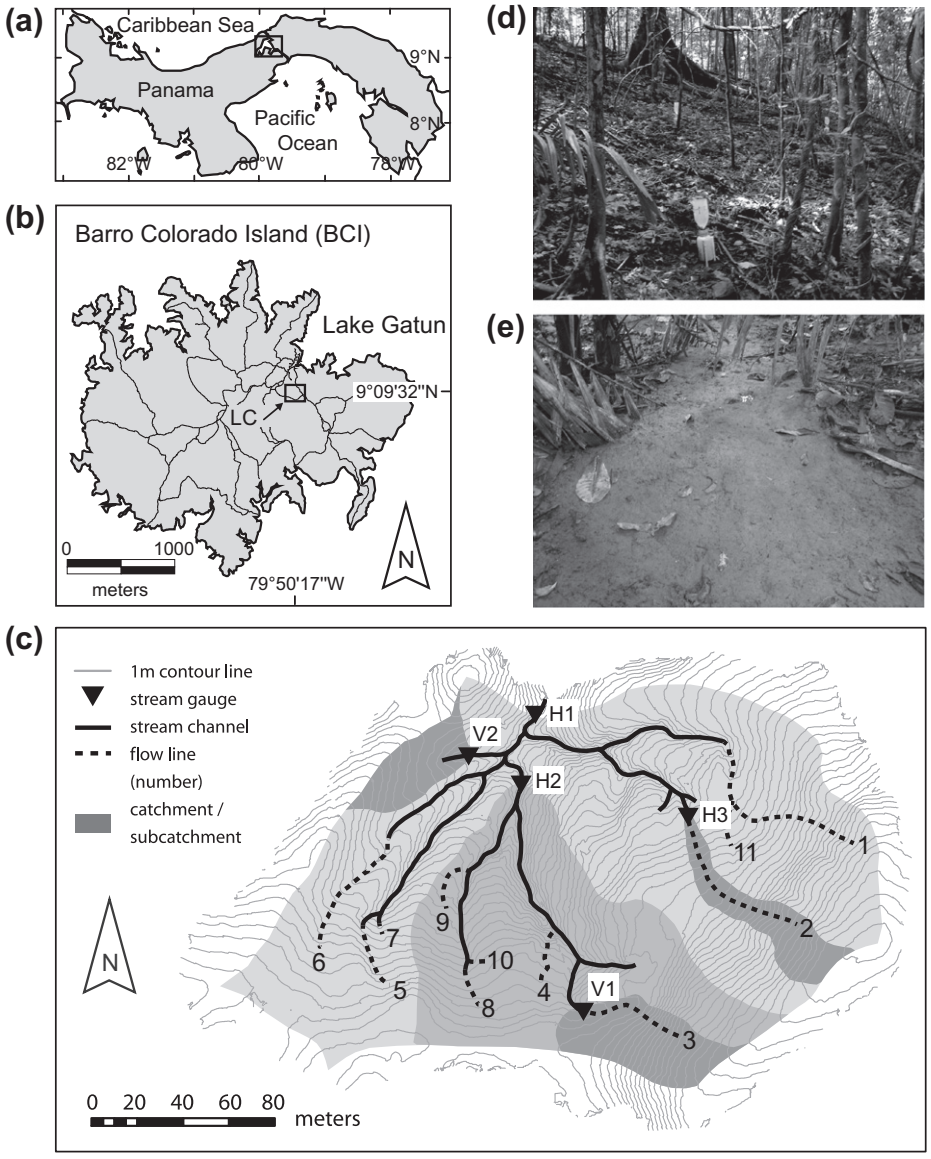

Fig. 2. Location of the research area in (a) Panama and (b) at Barro Colorado Island. (c) Sampling locations and catchment boundaries of Lutzito catchment (LC). Flow lines (numbered, dashed lines) mark areas where overland flow drains into the stream channel system (solid lines). (d) A view at a slope in LC. (e) Flow line #2 near the gauging site H3 shortly after rainfall.

Streamflow is intermittent and ceases usually in January due to low rainfall during the dry season (Fig. 3a) and the limited water storage capacity of LC. At the end of the dry season, the soils in LC show cracks up to 2 cm wide and 10 cm deep (Dietrich et al., 1982), due to the substantial admixture of smectite in the clay fraction (Grimm et al., 2008). The first rains saturate the soils quickly, cracks close and by July rainfall has increased the relative saturation in the upper soil to more than 60% (Fig. 3b). From that point onwards streamflow reacts extremely rapid to rainfall, which is reflected in a time to peak-value of 18 ± 10 min (mean ± 1 sd, n = 89 single peaked storm events, data from 2007 to 2009). An examination of soil physical properties in the study area reveals that we can safely rule out Horton-type overland flow because infiltrability values exceed rainfall intensities (infiltrability: 406.9 ± 157.5 mm h^{-1}, median ± MAD (median absolute deviation), n = 18; maximum 5-min rainfall intensity: 16.8 ± 12.0 mm h^{-1}, median ± MAD, n = 567 events, events are defined as rainfalls of at least 0.2 mm separated by a minimum dry period of 2 h). Soil permeability, however, decreases markedly at 20 cm depth (2.7 ± 2.6 mm h^{-1}, median ± MAD, n = 14, Fig. 4), which results in an impeding layer, given the prevailing rainfall characteristics (Fig. 4) and soil moisture conditions during the wet season (Fig. 3b). The pronounced soil anisotropy in LC, expressed in the marked decrease of permeability with depth, explains previous (Godsey et al., 2004; Loos and Elsenbeer, 2011) and our observations (Figs. 2e and 5; see also Video 1, Supplementary material) of frequent and widespread saturation excess overland flow.

2.2. Suspended-sediment sampling and monitoring of ancillary variables

We sampled suspended-sediment at five sites (Fig. 2c): at the catchment outlet (H1, 3.3 ha), in a subcatchment with permanent streamflow during the wet season (H2, 1.3 ha), at a site that usually receives overland flow during storms and limited baseflow during the late wet season (V2, 0.11 ha), and at two sites that solely receive overland flow (H3, 0.08 ha; and V1, 0.17 ha). We equipped the sampling sites with a 2 ft H-flume (H1), 1 ft H-flumes (H2

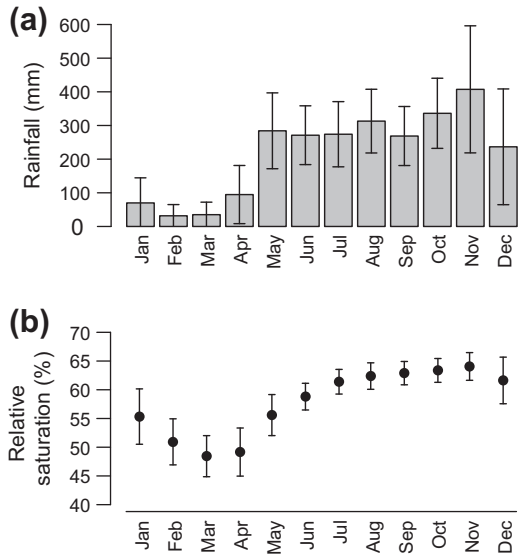

Fig. 3. Monthly rainfall (a) and relative (water) saturation in 0–10 cm depth (b) at the research site based on a 81 year rainfall record (1929–2009) and a 32 year soil moisture monitoring (n = 10 sites, 1972–2009), respectively. The bars indicate ±1 standard deviation.

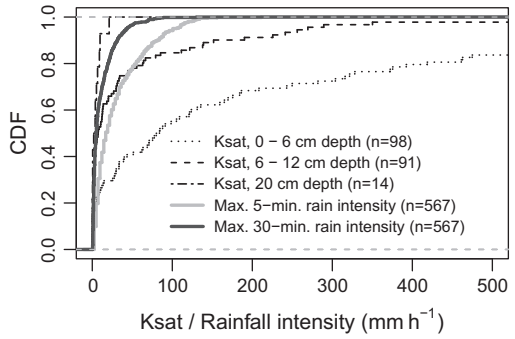

Fig. 4. Cumulative distribution functions (CDFs) of the saturated hydraulic conductivity in three soil depths (0–6, 6–12, and 20 cm) and CDF's of maximum 5-min and 30-min rainfall intensities based on all rainfall events that occurred during the study period (2007–2009, n = 567). Note that the majority of the recorded maximum rainfall intensities exceed the permeability in 20 cm depth.

and H3), and RBC-flumes (V1 and V2). At each sampling site we used automatic water samplers (ISCO 6712) for within-event monitoring. To capture the suspended-sediment dynamics at our sites we triggered the automatic sampling at relatively low discharges and sampled every 5 min for the first hour of an event, then 10 times in 10 min intervals, and finally ended sampling with a 60 min interval. Occasionally, however, we also took grab samples to cover baseflow, to improve coverage early on the rising limb, and to ensure sampling of multiple storms. All sediment samples were filtered through pre-weighed glass fiber filters with a nominal pore size of 1.6 µm (Whatman, GF/A). The filtrate was then oven-dried at 105 °C for 24 h and weighed. More details on the suspended-sediment data are provided in Table 1.

At each sampling site we recorded the water level at 5-min intervals with a bubbler flow module (ISCO 730) and a capacitive water stage sensor (Trutrack WT-HR). To ensure constant quality of the discharge record, all instruments were calibrated weekly. Discharge monitoring at H1, H2, and V2 started in October 2007, the other sites were established in early 2008. The discharge monitoring program operated until the end of 2009.

Finally, we measured rainfall with two Hobo tipping bucket rain gauges (orifice of 182 cm^2, 0.2 mm tip resolution) in a clearing 250 m from the catchment outlet. Tipping bucket data was checked against data obtained with five manual read out collectors (orifice of 113 cm^2) for 95 rainfall events. The latter test indicated that tipping buckets slightly underestimated rainfall. Therefore, we report either corrected event-based rainfall values or provide annual rainfall totals based on manual readouts (data provided by the Smithsonian Tropical Research Institute, Environmental Science Program). For our calculations, however, we used raw tipping bucket data due to their continuous availability and high resolution. These data contain no missing values and span the entire period from 2007 to 2009.

2.3. Modeling suspended-sediment concentration and estimation of sediment yields

2.3.1. Rationale for modeling suspended-sediment concentration using an ensemble tree approach

To check our conjecture posted in the introduction, the calculation of suspended-sediment yields (SSYs) is mandatory for two reasons: First, event-based and annual SSY can be used to assess the contribution of individual subcatchments to the SSY at the catchment outlet (H1, Fig. 2c). As three of the studied subcatchments (H3, V1, and V2) receive overland flow during storms, comparisons between these catchments and the outlet (H1) allow us to assess the role of overland flow as a driver of suspended-sediment transport. Second, annual SSY data serve as the basis for comparisons with other undisturbed forest ecosystems. These comparisons represent the necessary background data to judge if the estimated SSY at our site indeed rank at the higher end. For a reliable computation of SSY, continuous data of suspended-sediment concentrations (SSCs) are indispensable. To derive continuous SSC data series from intermittent SSC measurements (see Section 2.2), we employ a statistical model.

Traditionally, sediment rating curves (SRCs) have been used to derive continuous SSC data series (Walling, 1984), but alternative and more complex approaches such as fuzzy logic (Kisi et al., 2006), artificial neural networks (Nagy et al., 2002; Schnabel and Maneta, 2005) and various multivariate regression methods (Schnabel and Maneta, 2005; Francke et al., 2008a) exist. Standard SRCs rely on the assumption that discharge and SSC show a bijective relationship. At our monitoring sites, however, SSC correlated only weakly with discharge (Fig. 6) and pronounced hysteresis effects can be observed (Fig. 7). As a result, SRCs performed inadequately (Fig. 6), which is reflected in Nash–Sutcliffe-efficiency values (Nash and Sutcliffe, 1970) of around zero even for datasets comprising all observations. Because SRCs failed to capture the dynamics of SSC at our study site we had to choose an alternative approach.

Previous studies showed that antecedent rainfall and within-event discharge dynamics can strongly influence SSC (Ide et al., 2009; Smith and Dragovich, 2009). The latter influence becomes apparent in multiple peaked events as SSC during later event stages depend on the magnitude of the preceding hydrograph peak (cf. Fig. 3, Smith and Dragovich, 2009). This example illustrates that we can expect non-additive behavior (or non-linear behavior) in the discharge–SSC relationship. In other words, an increase in discharge is not necessarily reflected in increasing SSC. Moreover, usually both response variable (i.e. SSC) and predictor variables (e.g. discharge and rainfall) represent non-Gaussian data. Therefore, our SSC-models (one model for each monitoring site) have to account for the multitude of processes that control SSC (discharge dynamics, antecedent wetness conditions, etc.), need to deal with non-Gaussian data structure of predictor and response variables, and have to handle correlations between predictors. Quantile Regression Forest models (Meinshausen, 2006) are well suited for this task and have been successfully applied for SSC modeling (Francke et al., 2008a, 2008b).

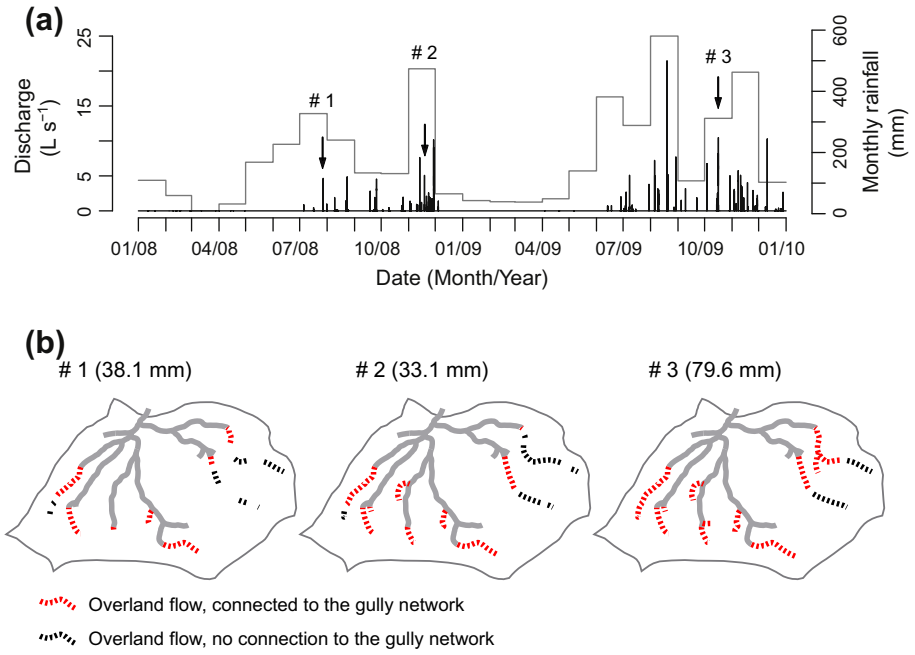

Fig. 5. Temporal frequency of overland flow measured at gauging site H3 (a), and spatial distribution (b) of overland for selected events of different antecedent moisture conditions and rainfall magnitudes (in parentheses). Gray solid lines refer to the gully network, whereas dashed lines illustrate parts of flowlines where overland flow was recorded by overland flow detectors (Kirkby et al., 1976). Events #1 and #2 illustrate the increasing connectivity of overland flow during the progressing wet season, and event #3 depicts a high connectivity situation typical for large, late wet season events.

Table 1
Characteristics of suspended-sediment concentration (SSC) data.

Sampling site	Number of samples	Number of events	SSC (g L^{-1})		
			Min	Mean	Max
H1	874	42	0.00	0.38	2.99
H2	124	7	0.00	0.23	1.29
H3	87	12	0.08	0.61	2.22
V1	103	9	0.07	0.75	2.96
V2	143	9	0.00	0.28	2.04

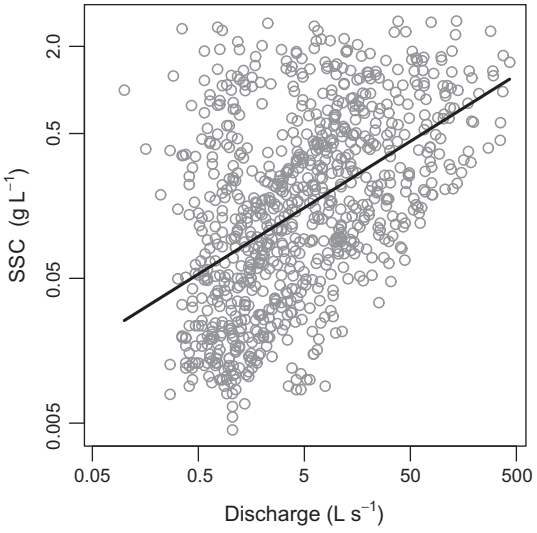

Fig. 6. Example of discharge–suspended-sediment concentration (SSC) relationship illustrated for the catchment outlet (H1). The black line refers to a sediment rating curve fitted to the log-transformed data.

Quantile Regression Forest (hereafter QRF) is a multivariate non-parametric regression technique that builds on Random Forest (RF) regression tree ensembles (Breiman, 2001). Regression trees, also known as Classification and Regression Trees (CARTs) (Breiman et al., 1984), are constructed by recursive data partitioning. RF and QRF employ an ensemble of these trees. Each tree consists of a number of decision nodes; at each node the training data (i.e. calibration data) are split into separate subsets so as to reduce the variance of each subset. This procedure is done until a predefined minimum node size has been reached. In RF and QRF individual trees of the forest ensemble are grown on a random subset of the training data. The procedure of employing only a subset of the training data to grow a tree is called "bagging" and the data not used for constructing the trees are termed "out of bag data". The idea of bagging is to average many noisy but approximately unbiased models (Hastie et al., 2009). Moreover, at each node a random selection of input variables is used to construct the split. The concept of random selection of input variables reduces the correlation between trees and thus further improves the robustness of the model. In RF, model estimates are based on the mean of all tree predictions, whereas QRF employs the whole distribution of tree predictions and hence, offers the possibility to assess the accuracy and precision of model estimates (Meinshausen, 2006). The latter feature of QRF models represents an advantage compared to other methods such as fuzzy logic and artificial neural networks that do not provide error estimates of the predictions (Francke et al., 2008a).

For calculations and model building, we used the software R, version 2.10.0 (R Development Core Team, 2009) and here primarily the packages randomForest (Liaw and Wiener, 2002) and quantregForest (Meinshausen, 2007). We ran our QRF models using default parameter values (Liaw and Wiener, 2002; Meinshausen, 2007): the number of variables selected at each node was set to p/3, where p is the total number of variables, the minimum node size was set to 5, and the number of trees was set to 500.

2.3.2. Variables

With our modeling we aimed to acknowledge the highly dynamic nature of SSC in small streams and to consider the influence of antecedent conditions. To achieve the first issue we modeled at 5-min resolution, a high temporal frequency, predetermined by the maximum resolution of our rainfall and discharge data. To realize our second aim we constructed ancillary predictors, P_n, derived from primary predictors P (i.e. rainfall and discharge) by using increasing temporal shifts and window sizes, S_n, which allowed the description of past hydrometeorological conditions while keeping correlation between the derived predictors as low as possible:

$$S_n = \begin{cases} a_0 \sum_{i=0}^{n} q^i & \forall n \geqslant 0 \\ 0 & n = -1 \end{cases}, \quad (1)$$

$$P_n(t) = \sum_{i=S_{n-1}+a_0}^{S_n} P(t+i), \quad (2)$$

where a_0 denotes the temporal resolution of the rainfall and discharge time series, q is the growth factor for the temporal shifts and window sizes, and n denotes the respective time period. For our SSC predictions we used nine levels of S_n ($n = 0, 1, 2, \ldots, 8$) for rainfall and five levels of S_n ($n = 0, 1, 2, \ldots, 4$) for discharge, which corresponds to pre-event periods of 34 days and 10 h (given $q = 3$, and $a_0 = 5$ min), respectively. As additional predictors, we used the day of year to capture the pronounced seasonality (Fig. 3a) and the change in discharge as a useful indicator for intra-event dynamics. The procedure to obtain ancillary variables described above yields predictors that contain discrete portions of information, which reduces multi-collinearity and allows a clearer identification of variable importance compared to the mere aggregation of different window sizes (as e.g. in Francke et al., 2008a).

We assessed the variable importance, VI, with a permutation-based measure (Liaw and Wiener, 2002). The VI of a predictor P is calculated as the difference d between mean square error (MSE) of the predictions for each tree t, with $t \in \{1, \ldots, ntree\}$, and the MSE of the predictions with permuted values of a predictor P^*. In both cases, prediction performance is assessed on "out of bag data" (OOB, data not used for modeling). The differences in MSE, d, are then averaged over all trees and normalized by the standard error:

$$\mathrm{VI} = \frac{\frac{1}{ntree}\sum_{n=1}^{ntree} d}{\frac{\sigma(d)}{\sqrt{ntree}}}, \quad (3)$$

$$d = \mathrm{MSE}_{OOB}^{t,P*} - \mathrm{MSE}_{OOB}^{t,P}, \quad (4)$$

$$\mathrm{MSE}_{OOB} = \frac{\sum_{i=1}^{n} [\mathrm{SSC}_{obs}(i) - \mathrm{SSC}_{mod}(i)]^2}{n}, \quad (5)$$

where SSC_{obs} and SSC_{mod} refer to observed and modeled SSC values, and n refers to the number of records in the out of bag data. Predictors with low importance have a low impact on model quality, and hence show relatively small VI values. In order to compare the influence of predictors among all monitoring sites we normalized VI to 100%.

2.3.3. Validation

To validate our SSC predictions we applied the Nash–Sutcliffe-efficiency index, NSE (Nash and Sutcliffe, 1970):

$$\mathrm{NSE} = 1 - \frac{\sum_{i=1}^{n} [\mathrm{SSC}_{obs}(i) - \mathrm{SSC}_{mod}(i)]^2}{\sum_{i=1}^{n} [\mathrm{SSC}_{obs}(i) - \overline{\mathrm{SSC}_{obs}}]^2} \quad (6)$$

where the subscripts '*obs*', and '*mod*' refer to observed and modeled SSC values, respectively, and $\overline{\mathrm{SSC}_{obs}}$ is the mean of observed SSC values. Modeled SSC values are mean values of all tree predictions ($n = 500$) from the QRF model for the respective time step i.

The validation procedure usually involves several arbitrary decisions such as the definition of the size of the test data set and its location. We avoided both decisions by varying the size of the test data set (i.e. validation data not used for training the model) in fractions from 10% to 50% of the total data set and by calculating NSE values for all possible choices of the test data with training or test data in temporally contiguous blocks. For the final SSC modeling and calculation of annual sediment yields we used the full data sets.

2.3.4. Estimation of suspended-sediment yields and assessment of their precision

We computed suspended-sediment yields (SSYs) applying a Monte Carlo approach (Francke et al., 2008a): For each 5-min time-step we randomly drew a SSC prediction from the distribution of single tree predictions obtained with the QRF model. Based on these SSC data we calculated event-based and annual SSY, and by repeating this procedure 100 times for the respective intervals we obtained a distribution of SSY estimates. After confirming the Gaussian shape of the SSY distributions, we used the mean and the standard deviation as measure of central tendency and spread, respectively. The spread of the SSY estimates, which is influenced by the spread of the SSC predictions, can then be used to assess the precision of the SSY estimates.

The random drawing of predicted SSC values described above assumes uncorrelated model errors, e, defined here as the absolute differences between observed and predicted values. We verified this assumption by analyzing the temporal correlation of e using variograms according to Zimmermann et al. (2009).

3. Results

3.1. Modeling suspended-sediment concentration

3.1.1. Predictors

Our analysis of variable importance (Fig. 8) indicates that predictors containing hydrological information from a time span of 1 h prior the SSC prediction are most influential. The latter result is valid for all sampling sites and reflects the fast hydrological response to rainfall at the research site. Nevertheless, at the catchment outlet (H1), the day of year, a predictor related to annual dynamics, is also of importance. At this gauging site, substantial stormflow occurs early in the wet season and SSC display an annual trend; that is, maximum SSC during early wet season events tend to be lower than in events of similar magnitude later in the season. At the other sampling sites, stormflow occurs frequently only after the soils are saturated; hence, SSC samples from the early wet season are sparse and intra-seasonal dynamics are difficult to detect.

Though our approach to derive ancillary predictors (Eqs. (1) and (2)) increased the interpretability of predictors, it remains difficult to assess the influence of individual variables in more detail. That is to say, the explanatory power of the variable importance has its limitations because the importance of a variable may result from complex interactions with other variables (Liaw and Wiener, 2002). Therefore, we did not attempt to reduce the number of variables by omitting those of lower importance.

3.1.2. Validation

The validation of our models by means of Nash–Sutcliffe-efficiency indices (Table 2) indicates that the QRF model for the catchment outlet (H1), which builds on the largest data set, shows a satisfactory performance. Surprisingly, results for the V2 site are

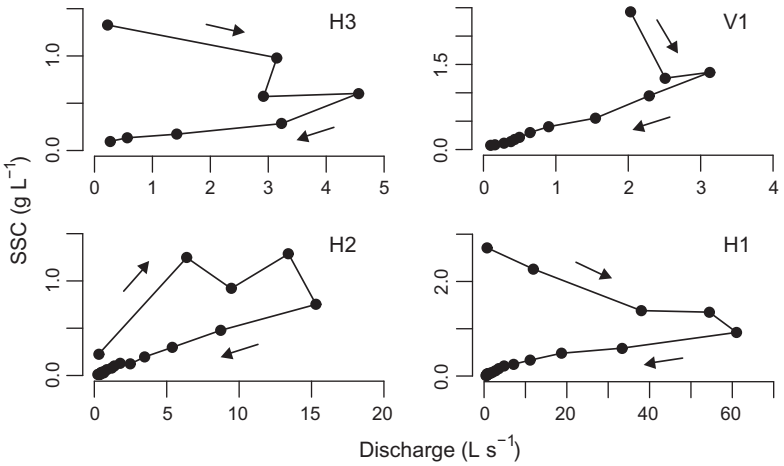

Fig. 7. Examples of hysteresis patterns of suspended-sediment concentrations, which were measured simultaneously at overland flow (H3 and V1) and streamflow (H2 and H1) sampling sites during an event in September 2008.

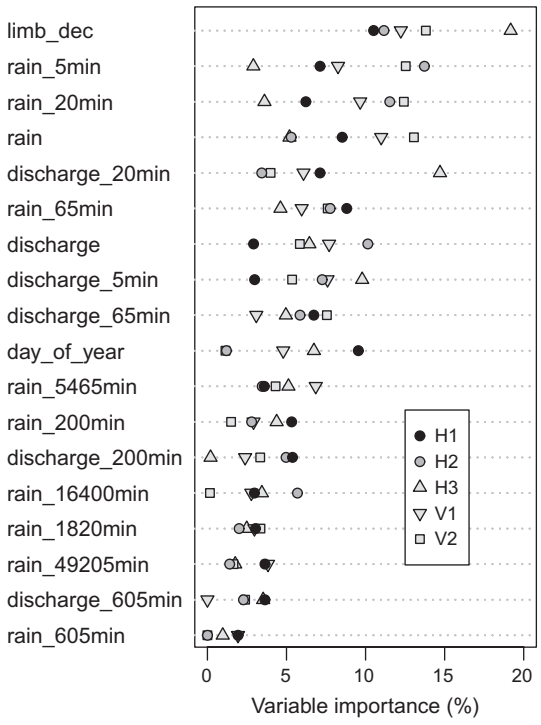

Fig. 8. Variable importance of SSC predictions for each monitoring site (H1, H2, H3, V1 and V2) normalized to 100%. Abbreviations are as follows: limb_dec, change in discharge; rain_min and discharge_min, cumulated rainfall and discharge for respective temporal shift and window size, S_n (see Eqs. (1) and (2) for the definition of temporal shifts and window sizes).

almost as good as for the main gauging site despite the smaller size of the training data set (Table 1). Model results for all other sites are less robust, particularly at the sampling site V1 whose low NSE values we attribute to a somewhat lower quality of the SSC data; data quality is determined by the total number of samples, the number of events, and the quantity of samples taken by hand (capturing situations not covered by the automatic sampling). Hence, characteristics of the training data (Table 1) mostly explain the observed differences in model performance and robustness (Table 2).

Varying the size of test data blocks and their position in the data set reveals not only the influence of test data characteristics on the validation procedure but also helps to assess local model performance. In general, large test data blocks average out local minima of model performance, which hampers the detection of prediction problems for specific events (Fig. 9). The positioning of the test data block seems to be another critical point in the validation procedure. For example, the QRF model for the main gauging site (H1) provides the best results for events sampled during the progressing wet season (NSE values of up to 0.94), whereas SSC predictions for early wet season events are less optimal (Fig. 9). Particularly, the test data set with the smallest block size (i.e. 10% of the total data set) shows a pronounced drop of prediction quality, which is related to the inclusion of an early wet season event in the test data. This event was unique and showed difficult to predict SSC dynamics as it was the first large (June 9th, 86.5 mm) rain in the 2008 wet season, which triggered, despite its magnitude, only limited overland flow (e.g. no overland flow signal at gauging site H3, Fig. 5a). During this event, most of the water drained into soil cracks and observed SSC at the catchment outlet were relatively low (maximum SSC: 0.39 g L^{-1}, cf. Table 1 for SSC statistics). Excluding these SSC data from the training data set results in an overestimation of SSC; and hence, explains the poor model performance at this point (Fig. 9).

So far we examined model performance based on test data blocks. Next we look at modeled and observed SSC dynamics during a single exemplary event. Although QRF model predictions capture SSC dynamics for both overland flow (Fig. 10b) and streamflow sampling sites (Fig. 10d), both graphs also show the limitations of our models: model predictions are particularly uncertain at the beginning of events, which is reflected in the large range of SSC predictions from the QRF tree ensemble (Fig. 10b and d, e.g. at time 17:10). Furthermore, at all overland flow sites SSC predictions show a somewhat larger uncertainty (i.e. a lower accuracy and precision) at the end of events (Fig. 10b, time period: 17:55–18:30). The elevated uncertainty of SSC predictions during the aforementioned situations is related to limited training data availability. During stormflow conditions, however, SSC predictions match field observations well (Fig. 10b and d), which is crucial regarding the estimation of sediment yields.

3.2. Suspended-sediment yield

3.2.1. Event-based comparisons

A plot of event-based suspended-sediment yields (SSYs) at the main gauging site against SSY of the subcatchments (Fig. 11) shows that apart from three major events, SSY of the overland flow

Table 2
Validation of SSC predictions by means of Nash–Sutcliffe-efficiency indices, NSE, for all possible positions of contiguous test data and various fractions of training and test data (NSE_{train} and NSE_{test}, respectively). The NSE's are median values of all positions of test data for the respective fractions.

Sampling site	Full dataset	Fraction of test data									
		10%		20%		30%		40%		50%	
	NSE_{train}	NSE_{train}	NSE_{test}	NSE_{train}	NSE_{test}	NSE_{train}	NSE_{test}	NSE_{train}	NSE_{test}	NSE_{train}	NSE_{test}
H1	0.95	0.95	0.76	0.95	0.73	0.95	0.71	0.95	0.68	0.95	0.67
H2	0.90	0.91	0.58	0.90	0.66	0.90	0.68	0.90	0.67	0.90	0.64
H3	0.87	0.86	0.59	0.86	0.52	0.85	0.48	0.84	0.42	0.84	0.36
V1	0.87	0.86	0.36	0.85	0.33	0.84	0.28	0.83	0.16	0.81	0.10
V2	0.90	0.90	0.72	0.89	0.71	0.89	0.65	0.87	0.68	0.86	0.57

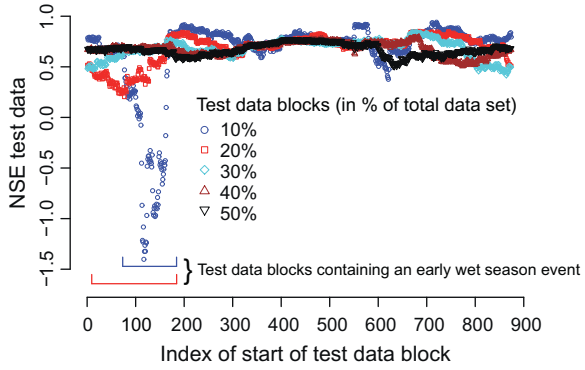

Fig. 9. Validation of QRF model predictions (exemplarily shown for the main gauging site H1), by means of the Nash–Sutcliffe efficiency indices for various sizes of test data blocks and all possible positions of test data within the data set. The smallest test data fraction (blue circles) shows a pronounced drop of NSE values, whereas NSE values of the other test data fractions display either a comparably small decrease (20% test data fraction, red squares), or show no decrease of NSE values at this point (test data fractions $\geqslant$30%). The brackets at the bottom of the plot indicate which of the 10% (blue bracket) and 20% test data blocks (red bracket) contain an early wet season event which showed difficult to predict SSC dynamics.

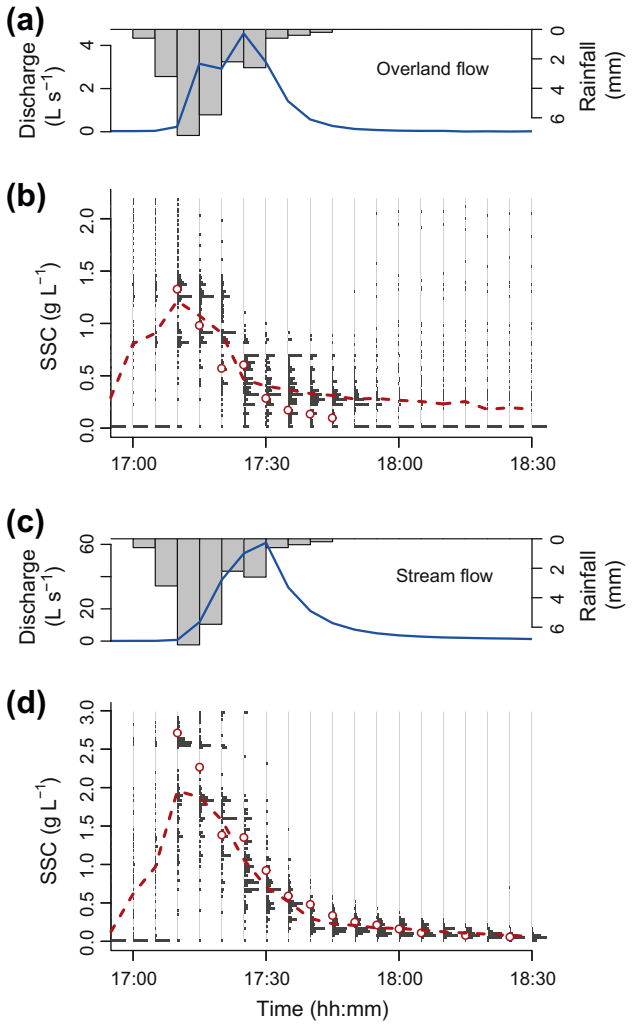

Fig. 10. Examples of overland flow (a), streamflow (c), and suspended-sediment concentration (SSC) dynamics (b and d) at the sampling site H3 (a and b) and at the main gauging site H1 (c and d) during an event in September 2008. The gray horizontal bars in the graphs (b and d) show SSC predictions of the QRF model for each time step, the red dashed line indicates the mean of these predictions. Modeled SSC values were obtained using 90% of the data set as training data, i.e. excluding the observations during the depicted event (red empty circles).

sampling sites (H3 and V1) match and sometimes even exceed SSY at the catchment outlet (H1). The SSY at our third overland flow sampling site (V2) show a similar pattern even though this site has some baseflow during the late wet season.

For three large ($\geqslant$80 mm) and high intensity (5-min intensities of up to 187 mm h^{-1}) rainfall events, however, SSY at the main gauging site (H1) exceed SSY of all subcatchments (Fig. 11). During one of those events, we observed stream bank failures only few meters upstream of gauging site H1. Increasing erosion of the stream channel during large events may explain the larger SSY at the catchment outlet. The ratios of the SSY during these events, however, vary a lot: SSY at overland flow sampling site H3 are only slightly below the SSY of the catchment outlet (H1), whereas SSY at the other sampling sites (V1, V2 and H2) are often clearly lower (Fig. 11). The latter result shows that suspended-sediment source areas are spatially not uniformly distributed; furthermore, source areas seem to vary temporally. For example, during two of the largest events, SSY at overland flow sampling site H3 clearly exceed the yield of the nearby sampling site V1, whereas the opposite is true for the majority of the remaining events (cf. upper graphs of Fig. 11).

3.2.2. Annual budgets

The spatial heterogeneity of SSY already visible in the event-based budgets (Fig. 11) manifests itself in pronounced differences in annual SSY among sampling sites (Fig. 12). Moreover, differences between the dry year 2008 (annual rainfall: 1975 mm) and the wetter following year (annual rainfall: 2544 mm) become apparent. For 2008, one of the driest years in the 81 year record, the SSY for the catchment outlet amounts to 1 t ha^{-1}. In 2009, a year with average rainfall, we estimated a SSY of 2 t ha^{-1} for the same sampling site (Fig. 12). All subcatchments also show an increasing SSY in 2009, albeit to a varying degree. The observed differences of annual SSY for the three overland flow sampling sites (H3, V1 and V2) are related to their distinct hydrological response to rainfall. That is, the duration of stormflow at sampling site H3

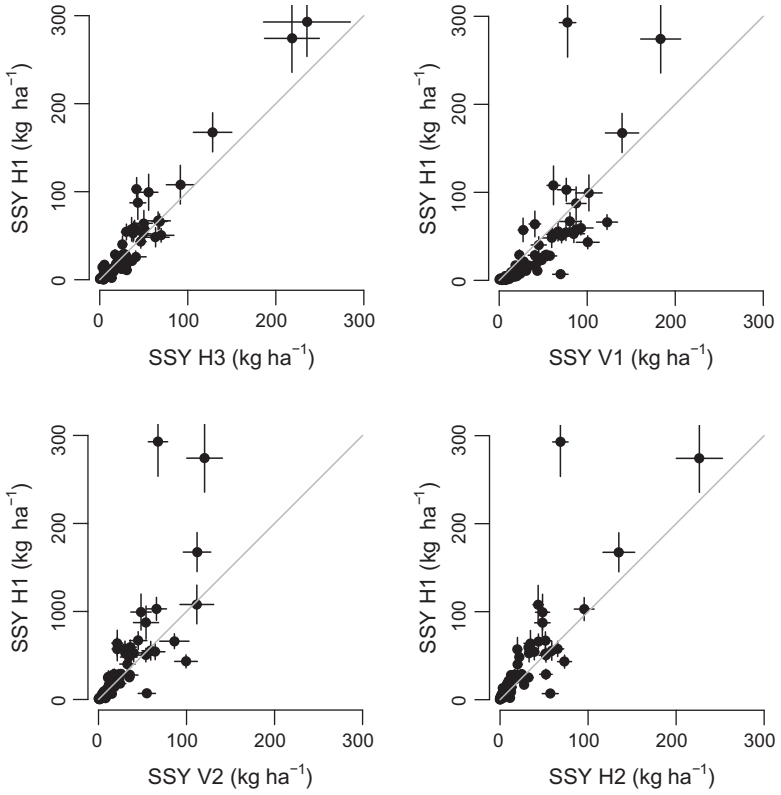

Fig. 11. Suspended-sediment yield (SSY) at the catchment outlet (H1) plotted against SSY at the subcatchment sampling sites (H3, V1, V2 and H2) for 74 rainfall events which occurred during the monitoring years 2008–2009. The bars indicate ±1 standard deviation, and the gray line illustrates a 1:1 ratio of sediment yield. The selected events triggered a hydrological response at all sites. Suspended-sediment yields are based on 6 h periods starting at the onset of rainfall. This time period covers stormflow sediment dynamics at all sites and for all selected events, respectively.

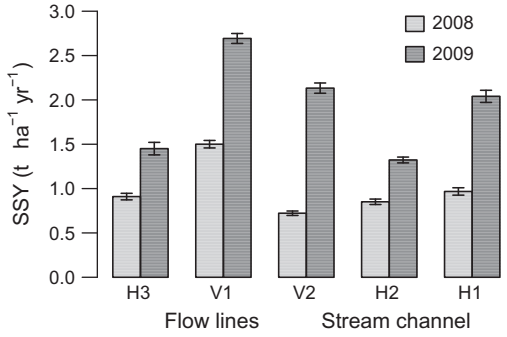

Fig. 12. Annual suspended-sediment yield (SSY) for 2008 and 2009 at four subcatchments (H3, V1, V2 and H2) and the catchment outlet (H1). The monitoring sites H3 and V1 receive only overland flow, site V2 is dominated by overland flow but baseflow occurs occasionally during the late wet season, whereas sites H2 and H1 show permanent streamflow throughout the wet season.

differs only slightly between 2008 and 2009, whereas stormflow at sampling sites V1 and V2 increased substantially.

The precision of our annual SSY estimates (Fig. 12) seems somewhat surprising, particularly when compared to the event-based estimates (Fig. 11). In situations where SSY budgets are calculated for long time periods, however, the influence of predictions with a low precision (indicating a large predictive uncertainty at these points) is averaged out. This effect partly explains the low spread, and hence the high precision, of the annual SSY estimates (Fig. 12). Nevertheless, the low spread of the SSY estimates also indicates that the SSC predictions are particularly precise during periods most relevant for suspended-sediment exports, i.e. during high discharge conditions (Fig. 10).

4. Discussion

4.1. Forests and erosion: contradiction in terms?

There are many situations where the interplay between soil and rainfall characteristics triggers near-surface lateral flow in forest ecosystems. Given sufficiently large rainfall intensities or amounts, soil characteristics such as a low permeability at a shallow depth (Bonell and Gilmour, 1978; Elsenbeer and Vertessy, 2000; Godsey et al., 2004), a low water-storage capacity owing to a shallow soil mantle (Allan and Roulet, 1994), or hydrophobic conditions at the soil surface (Gomi et al., 2008; Ide et al., 2008) cause the activation of overland flow. Our data (Figs. 4, 5, and 10a) and field observations (Fig. 2d; Video 1, Supplementary material) add to the wealth of evidence (Fig. 1) that overland flow may occur frequently in undisturbed forest environments. Acknowledging the latter phenomenon, and given that the activation of (near) surface flowpaths is not restricted to a few sites as supposed by Sidle et al. (2006), we suggest to rethink the common belief that considers erosion in undisturbed forest ecosystems as negligible (e.g. Bruijnzeel, 2004; Sidle et al., 2006).

Our observations and measurements provide evidence that overland flow relocates leaf litter (Fig. 2d) and transports loose soil material (Figs. 10b, 11, and 12). The transport of soil material probably accelerates during the progressing wet season due to a positive feedback mechanism. The first rains remove the leaf litter in flowlines while transporting relatively little soil. Subsequent events carry increasing amounts of fine soil material which seals macropores in the flowlines. Both processes promote an efficient transport of material from the hillslopes, which is reflected in the large sediment yields of the overland flow monitoring sites (Figs.

11 and 12). Additionally, major rainfalls cause substantial stormflow, which triggers localized streambank failure (field observations). During these high-connectivity events (e.g. event #3, Fig. 5b), some hillslopes (Fig. 11) lose more than 200 kg ha^{-1} of suspended-sediment, and up to 300 kg ha^{-1} of suspended-sediment leave the catchment (Fig. 11). These numbers indicate that a well developed tree cover is not necessarily capable of preventing surface erosion.

4.2. Site comparisons: do sediment yields reflect the frequency of near-surface flow?

Our SSY estimates rank high when compared with data from other undisturbed forest catchments (Table 3). Indeed, only two sites, both located in Danum Valley, Malaysian Borneo, show SSY similar (Sayer et al., 2006b) to or even higher (Douglas et al., 1992) than ours. At those sites, overland flow also occurs frequently (Sinun et al., 1992; Clark and Walsh, 2006; Sayer et al., 2006b), though its spatial extent is still not entirely known (Clark and Walsh, 2006). We suppose that differences between SSY at Danum Valley and our 2009 data (a year of average rainfall at our site) reflect a distinct hydrological functioning. At Danum Valley, both overland flow and pipe flow occur (Chappell, 2010; Sayer et al., 2006b), and collapsing pipe systems create additional sediment source areas (Sayer et al., 2006b). This process is not relevant in our research area, which could explain the lower SSY value at our site. Alternatively, the observed difference may simply reflect differences in the number of large, high intensity rainfall events, which have a considerable influence on annual sediment yields (Douglas et al., 1999).

The lower suspended-sediment yields at other forested sites (Table 3) can be related to the spatial restriction of sediment source areas (Ide et al., 2009), to a low spatial and temporal frequency of overland flow (Godsey et al., 2004), or to the absence of near-surface flowpaths (e.g. Baharuddin, 1988; Grayson et al., 1993; Swank et al., 2001). Particularly sites of the latter category show extremely small annual sediment yields, lower even than the amount of suspended-sediment exported during single, frequently occurring events at our research site (cf. Table 3 and Fig. 11).

Our comparisons of SSY among undisturbed forest sites (Table 3) clearly indicate that hydrological characteristics strongly influence suspended-sediment dynamics in forested areas. In other words, although there is no doubt that vegetation reduces erosion to some degree (e.g. Rey, 2003; Bruijnzeel, 2004; Sidle et al., 2006), forests cannot impede erosion completely where a pronounced soil anisotropy (expressed as the change of the saturated hydraulic conductivity with depth) favors the activation of surface flowpaths. Our findings imply that relatively large SSY in forests are probably more common than previously thought given the actual bias of SSY studies towards vertical flowpath-dominated sites (Fig. 1).

4.3. Coupling and decoupling of overland flow and erosion: a hypothesis

Our discussion so far implicitly assumes that forests play a relatively passive role regarding erosion processes. This situation, however, is limited to certain boundary conditions: we hypothesize that a tight coupling of overland flow and erosion is restricted to areas without strong nutrient limitation, which is the case at our study site (Yavitt, 2000; Dieter et al., 2010) and its surroundings (Sayer et al., 2006a; Barthold et al., 2008; Dieter et al., 2010; Vincent et al., 2010). At these sites, trees do not build up thick root mats (Sayer et al., 2006a), and leaf litter contains enough nutrients to promote high decomposition rates (Kaspari and Yanoviak, 2009). In contrast, in strongly nutrient limited systems, particularly those limited in phosphorus, we anticipate that negative feedback mechanisms slow down erosion processes. That is to say, on nutrient-poor soils leaf litter is of low quality (Kaspari and Yanoviak, 2008, 2009), which is why decomposition is reduced (Hobbie and Vitousek, 2000; Kaspari and Yanoviak, 2009; Wieder et al., 2009), and as a consequence litter accumulates (Baillie et al., 2006; Kaspari and Yanoviak, 2008, 2009). Furthermore, root mats aid in absorbing nutrients (Stark and Jordan, 1978; Baillie et al., 2006). Both leaf litter and root mats dissipate the kinetic energy of throughfall (Geddes and Dunkerley, 1999; Baillie et al., 2006) and reduce erosion even in the presence of near-surface flow (Fukuyama et al., 2010).

The coupling of overland flow and erosion processes, however, depends not only on the nutrient status of the forest. We further hypothesize that light availability also influences erosion: Sparse canopies allow understory growth which effectively prevents sediment transport (Rey, 2003; Fukuyama et al., 2010). At our research site, canopy openness amounts to 3% (Zimmermann et al., 2009) and low vegetation is restricted to canopy gaps. These characteristics are unlikely to reduce sediment transport by overland flow (Figs. 10–12).

The natural setting at our research site does promote a strong coupling of overland flow and erosion. If our hypothesis holds, the trinity of frequent near-surface flow, relatively nutrient rich soils, and sparse ground vegetation represents a set of characteristics which could be used to identify erosion hot spots in forests.

Table 3
Selected undisturbed-forest sites for which information on both prevailing flowpaths and suspended-sediment data are available. Sites are arranged in ascending order of their sediment yield. When only one reference is given it provides data on flowpaths and SSY. *Abbreviations*: OF, overland flow; SSY, suspended-sediment yield.

Location	Overland flow, OF (absent = 0, present = 1)	Sediment yield, SSY (t ha^{-1} yr^{-1})	Reference OF; reference SSY
Australia	0	0.05	Grayson et al. (1993)
Malaysia	0	0.07	Chappell et al. (2005); Baharuddin (1988)
USA	0	0.14	Swank et al. (2001)
Malaysia	0	0.14	Chappell et al. (2005); Baharuddin (1988)
Malaysia	0	0.20	Chappell et al. (2005); Baharuddin (1988)
USA	0	0.23	Swank et al. (2001)
Malaysia	0	0.30	Malmer (1996)
Panama	1[a]	0.40	Godsey et al. (2004); Leigh (1999)
Japan	1	0.72	Ide et al. (2008); Ide et al. (2009)
Panama	1	0.97	This study (2008)
Malaysia	1	1.21[b]	Sayer et al. (2006b)
Panama	1	2.04	This study (2009)
Malaysia	1	3.12	Sinun et al. (1992); Douglas et al. (1992)

[a] Conrad Creek Catchment, with infrequent overland flow (Fig. 9, Godsey et al., 2004).
[b] The SSY budget based on a 9-month monitoring period.

Additional small catchment studies providing suspended-sediment yields, information on prevailing flow paths, data on forest structure, and soil nutrient status are necessary to test our hypothesis.

5. Conclusions

Forest cover and erosion rates as high as 2 t ha^{-1} yr^{-1} are no contradiction in terms where distinct soil anisotropy in shallow depth coincides with high rainfall intensities and amounts. Overland flow, which is frequently activated in the latter environment, acts as an important driver of erosion processes. Our observations indicate that during single, large rainfall events, overland flow-prone hillslopes lose more than 0.2 t ha^{-1} of suspended-sediment within hours, and the erosion of the stream channel further increases the catchment's event-based suspended-sediment yield to 0.3 t ha^{-1}. These findings do not only add to the wealth of knowledge that overland flow occurs in undisturbed forests but they also challenge the wide-spread belief that erosion rates are generally low under undisturbed forest cover.

Based on our results and using available background data from our study site, we hypothesize that undisturbed forest ecosystems are particularly susceptible to erosion where a trinity of active near-surface flowpaths, relatively nutrient rich soils (that coincide with sparse root mats), and a low light availability at the forest floor (preventing the growth of ground vegetation) exists. These conditions are probably more widespread than expected. In Panama, at least, they occur in extensive areas of the Panama Canal watershed.

Given that our monitoring period covered a dry (2008, annual rainfall: 1975 mm) and an average year (2009, annual rainfall: 2544 mm), it remains to be seen how extremely wet years with totals up to 4500 mm increase sediment yields.

Acknowledgements

This research was funded by the German Research Foundation (El 255/6-1). We thank Anna Schürkmann for participating in the field work. Furthermore, we are indebted to Oris Acevedo (Smithsonian Tropical Research Institute, STRI) for exceptional logistical support and to Sergio dos Santos (Terrestrial Environmental Sciences Program, STRI) for providing long-term rainfall and soil moisture data. Finally, we thank five anonymous reviewers for constructive comments on earlier drafts of this manuscript.

Appendix A. Supplementary material

Supplementary data associated with this article can be found, in the online version, at doi:10.1016/j.jhydrol.2012.01.039.

References

Allan, C.J., Roulet, N.T., 1994. Runoff generation in zero-order Precambrian Shield catchments: the stormflow response of a heterogeneous landscape. Hydrol. Process. 8, 369–388.

Badoux, A., Witzig, J., Germann, P.F., Kienholz, H., Lüscher, P., Weingartner, R., Hegg, C., 2006. Investigations on the runoff generation at the profile and plot scales, Swiss Emmental. Hydrol. Process. 20, 377–394. doi:10.1002/hyp.6056.

Baharuddin, K., 1988. Effect of logging on sediment yield in a hill dipterocarp forest in Peninsular Malaysia. J. Trop. Forest Sci. 1, 56–66.

Baharuddin, K., Abduhl Rahim, N., 1994. Suspended sediment yield resulting from selective logging practices in a small watershed in Peninsular Malaysia. J. Trop. Forest Sci. 7, 286–295.

Baillie, I.C., Ashton, P.S., Chin, S.P., Davies, S.J., Palmiotto, P.A., Russo, S.E., Tan, S., 2006. Spatial associations of humus, nutrients and soils in mixed dipterocarp forest at Lambir, Sarawak, Malaysian Borneo. J. Trop. Ecol. 22, 543–553. doi:10.1017/S026646740600352X.

Baillie, I., Elsenbeer, H., Barthold, F., Grimm, R., Stallard, R., 2007. Semi-detailed Soil Survey of Barro Colorado Island, Panama. Soil Report. <http://biogeodb.stri.si.edu/bioinformatics/bci_soil_map/index.php> (verified 22.09.10).

Barthold, F.K., Stallard, R.F., Elsenbeer, H., 2008. Soil nutrient–landscape relationships in a lowland tropical rainforest in Panama. Forest Ecol. Manage. 255, 1135–1148. doi:10.1016/j.foreco.2007.09.089.

Beschta, R.L., 1978. Long-term patterns of sediment production following road construction and logging in the Oregon Coast Range. Water Resour. Res. 14, 1011–1016.

Bonell, M., Gilmour, D.A., 1978. The development of overland flow in a tropical rainforest catchment. J. Hydrol. 39, 365–382.

Breiman, L., 2001. Random forests. Mach. Learn. 45, 5–32.

Breiman, L., Friedman, J., Olshen, R., Stone, C., 1984. Classification and Regression Trees. Wadsworth, Belmont, CA, USA.

Brown, G.W., Krygier, J.T., 1971. Clear-cut logging and sediment production in the Oregon Coast Range. Water Resour. Res. 7, 1189–1198.

Bruijnzeel, L.A., 2004. Hydrological functions of tropical forests: not seeing the soil for the trees? Agric. Ecosyst. Environ. 104, 185–228. doi:10.1016/j.agee.2004.01.015.

Chappell, N.A., 2010. Soil pipe distribution and hydrological functioning within the humid tropics: a synthesis. Hydrol. Process. 24, 1567–1581. doi:10.1002/hyp.7579.

Chappell, N.A., McKenna, P., Bidin, K., Douglas, I., Walsh, R.P.D., 1999. Parsimonious modeling of water and suspended sediment flux from nested catchments affected by selective tropical forestry. Philos. Trans. Roy. Soc. B – Biol. Sci. 354, 1831–1846.

Chappell, N.A., Tych, W., Yusop, Z., Rahim, N.A., Kasran, B., 2005. Spatially-significant effects of selective tropical forestry on water, nutrient and sediment flows: a modelling supported review. In: Bonell, M., Bruijnzeel, L.A. (Eds.), Forests, Water and People in the Humid Tropics: Past, Present and Future Hydrological Research for Integrated Land and Water Management. Cambridge University Press, Cambridge, UK, pp. 513–532.

Chatterjea, K., 1989. Surface wash: the dominant geomorphic process in the surviving rainforest of Singapore. Singapore J. Trop. Geogr. 10, 95–109.

Clark, M.A., Walsh, R.P.D., 2006. Long-term erosion and surface roughness change of rain-forest terrain following selective logging, Danum Valley, Sabah, Malaysia. Catena 68, 109–123. doi:10.1016/j.catena.2006.04.002.

de Moraes, J.M., Schuler, A.E., Dunne, T., Figueiredo, R.de O., Victoria, R.L., 2006. Water storage and runoff processes in plinthic soils under forest and pasture in Eastern Amazonia. Hydrol. Process. 20, 2509–2526. doi:10.1002/hyp.6213.

Dieter, D., Elsenbeer, H., Turner, B.L., 2010. Phosphorus fractionation in lowland tropical rainforest soils in central Panama. Catena 82, 118–125. doi:10.1016/j.catena.2010.05.010.

Dietrich, W.E., Windsor, D.M., Dunne, T., 1982. Geology, climate, and hydrology of Barro Colorado Island. In: Leigh, E.G., Rand, S.A., Windsor, D.M. (Eds.), The Ecology of a Tropical Forest: Seasonal Rhythms and Long Term Changes. Smithsonian Institution, Washington, DC, pp. 21–46.

Douglas, I., 1999. Hydrological investigations of forest disturbance and land cover impacts in South-East Asia: a review. Philos. Trans. Roy. Soc. B – Biol. Sci. 354, 1725–1738.

Douglas, I., Bidin, K., Balamurugan, G., Chappell, N.A., Walsh, R.P.D., Greer, T., Sinun, W., 1999. The role of extreme events in the impacts of selective tropical forestry on erosion during harvesting and recovery phases at Danum Valley, Sabah. Philos. Trans. Roy. Soc. B – Biol. Sci. 354, 1749–1761.

Douglas, I., Spencer, T., Greer, T., Bidin, K., Sinun, W., Meng, W.W., 1992. The impact of selective commercial logging on stream hydrology, chemistry and sediment loads in the Ulu Segama rain forest, Sabah, Malaysia. Philos. Trans. Roy. Soc. B – Biol. Sci. 335, 397–406.

Dykes, A.P., Thornes, J.B., 2000. Hillslope hydrology in tropical steeplands in Brunei. Hydrol. Process. 14, 215–235.

Elsenbeer, H., 2001. Hydrologic flowpaths in tropical rainforest soilscapes – a review. Hydrol. Process. 15, 1751–1759. doi:10.1002/hyp.237.

Elsenbeer, H., Vertessy, R.A., 2000. Stormflow generation and flowpath characteristics in an Amazonian rainforest catchment. Hydrol. Process. 14, 2367–2381.

Foster, R.B., Brokaw, N.V.L., 1982. Structure and history of the vegetation of Barro Colorado Island. In: Leigh, E.G., Rand, S.A., Windsor, D.M. (Eds.), The Ecology of a Tropical Forest: Seasonal Rhythms and Long Term Changes. Smithsonian Institution, Washington, DC, pp. 67–81.

Francke, T., López-Tarazón, J.A., Schröder, B., 2008a. Estimation of suspended sediment concentration and yield using linear models, random forests and quantile regression forests. Hydrol. Process. 22, 4892–4904. doi:10.1002/hyp.7110.

Francke, T., López-Tarazón, J.A., Vericat, D., Bronstert, A., Batalla, R.J., 2008b. Flood-based analysis of high-magnitude sediment transport using a non-parametric method. Earth Surf. Process. Landf. 33, 2064–2077. doi:10.1002/esp.1654.

Fritsch, J.M., Sarrailh, J.M., 1986. Les transports solides dans l'écosystème forestier tropical humide guyanais: effets du défrichement et de l'aménagement de pâturages. Cah. ORSTOM, sér. Pédol. 22, 209–222.

Fukuyama, T., Onda, Y., Gomi, T., Yamamoto, K., Kondo, N., Miyata, S., Kosugi, K., Mizugaki, S., Tsubonuma, N., 2010. Quantifying the impact of forest management practice on the runoff of the surface-derived suspended sediment using fallout radionuclides. Hydrol. Process. 24, 596–607. doi:10.1002/hyp.7554.

Garzía-Ruiz, J.M., Regüés, D., Alvera, B., Lana-Renault, N., Serrano-Muela, P., Nadal-Romero, E., Navas, A., Latron, J., Martí-Bono, C., Arnáez, J., 2008. Flood generation and sediment transport in experimental catchments affected by land use changes in the central Pyrenees. J. Hydrol. 356, 245–260. doi:10.1016/j.jhydrol.2008.04.013.

Geddes, N., Dunkerley, D., 1999. The influence of organic litter on the erosive effects of raindrops and of gravity drops released from desert shrubs. Catena 36, 303–313.

Germer, S., Neill, C., Krusche, A.V., Elsenbeer, H., 2010. Influence of land-use change on near-surface hydrological processes: undisturbed forest to pasture. J. Hydrol. 380, 473–480. doi:10.1016/j.jhydrol.2009.11.022.

Grimm, R., Behrens, T., Märker, M., Elsenbeer, H., 2008. Soil organic carbon concentrations and stocks on Barro Colorado Island – dgital soil mapping using Random Forests analysis. Geoderma 146, 102–113. doi:10.1016/j.geoderma.2008.05.008.

Godsey, S., Elsenbeer, H., Stallard, R., 2004. Overland flow generation in two lithologically distinct rainforest catchments. J. Hydrol. 295, 276–290. doi:10.1016/j.jhydrol.2004.03.014.

Gökbulak, F., Serengil, Y., Özhan, S., Özyuvacı, N., Nihat Balcı, A., 2008. Relationship between streamflow and nutrient and sediment losses from an oak-beech forest watershed during an 18-year long monitoring study in Turkey. Eur. J. Forest Res. 127, 203–212. doi:10.1007/s10342-007-0195-1.

Gomi, T., Sidle, R.S., Miyata, S., Kosugi, K., Onda, Y., 2008. Dynamic runoff connectivity of overland flow on steep forested hillslopes: scale effects and runoff transfer. Water Resour. Res. 44, W08411. doi:10.1029/2007WR005894.

Grayson, R.B., Haydon, S.R., Jayasuriya, M.D.A., Finlayson, B.L., 1993. Water quality in mountain ash forests – separating the impacts of roads from those of logging operations. J. Hydrol. 150, 459–480.

Hastie, T., Tibshirani, R., Friedman, J., 2009. The Elements of Statistical Learning. Springer, New York, NY, USA, pp. 587–604. doi: 10.1007/b94608_15.

Hobbie, S.E., Vitousek, P.M., 2000. Nutrient limitation of decomposition in Hawaiian forests. Ecology 81, 1867–1877.

Ide, J., Haga, H., Chiwa, M., Otsuki, K., 2008. Effects of antecedent rain history on particulate phosphorus loss from a small forested watershed of Japanese cypress (*Chamaecyparis obtusa*). J. Hydrol. 352, 322–335. doi:10.1016/j.jhydrol.2008.01.012.

Ide, J., Kume, T., Wakiyama, Y., Higashi, N., Chiwa, M., Otsuki, K., 2009. Estimation of annual suspended sediment yield from a Japanese cypress (*Chamaecyparis obtusa*) plantation considering antecedent rainfalls. Forest Ecol. Manage. 257, 1955–1965. doi:10.1016/j.foreco.2009.02.011.

Johnson, M.S., Lehmann, J., Couto, E.G., Filho, J.P.N., Riha, S.J., 2006. DOC and DIC in flowpaths of Amazonian headwater catchments with hydrological contrasting soils. Biogeochemistry 81, 45–57. doi:10.1007/s10533-006-9029-3.

Kaspari, M., Yanoviak, S.P., 2008. Biogeography of litter depth in tropical forests: evaluating the phosphorus growth rate hypothesis. Funct. Ecol. 22, 919–923. doi:10.1111/j.1365-2435.2008.01447.x.

Kaspari, M., Yanoviak, S.P., 2009. Biogeochemistry and the structure of tropical brown food webs. Ecology 90, 3342–3351. doi:10.1890/08-1795.1.

Kenoyer, L.A., 1929. General and successional ecology of the lower tropical rain-forest at Barro Colorado Island, Panama. Ecology 10, 201–222.

Kirkby, M., Callan, J., Weyman, D., Wood, J., 1976. Measurement and Modelling of Dynamic Contributing Areas in Very Small Catchments. Working Paper No. 167, School of Geography University of Leeds, Leeds, 39 pp.

Kisi, O., Karahan, M.E., Sen, Z., 2006. River suspended sediment modelling using a fuzzy logic approach. Hydrol. Process. 20, 4351–4362. doi:10.1002/hyp.6166.

Lal, R., 1983. Soil erosion in the humid tropics with particular reference to agricultural land development and soil management. In: R. Keller (Ed.), Hydrology of Humid Tropical Regions with Particular Reference to the Hydrological Effects of Agriculture and Forestry Practice. IHAS Publ. No. 140, Institute of Hydrology, Wallingford, UK, pp. 221–239.

Leigh, E.G., 1999. Tropical Forest Ecology. Oxford University Press, New York.

Lesack, L.F.W., 1993. Water balance and hydrologic characteristics of a rain forest catchment in the Central Amazon Basin. Water Resour. Res. 29, 759–773.

Liaw, A., Wiener, M., 2002. Classification and regression by randomForest. R News 2 (3), 18–22.

Loos, M., Elsenbeer, H., 2011. Topographic controls on overland flow generation in a forest – an ensemble tree approach. J. Hydrol. 409, 94–103. doi:10.1016/j.jhydrol.2011.08.002.

Malmer, A., 1996. Hydrological effects and nutrient losses of forest plantation establishment on tropical rainforest land in Sabah, Malaysia. J. Hydrol. 174, 129–148.

Meinshausen, N., 2006. Quantile regression forests. J. Mach. Learn. Res. 7, 983–999.

Meinshausen, N., 2007. quantregForest: Quantile Regression Forests. R Package Version 0.2-2.

Nagy, H.M., Watanabe, K., Hirano, M., 2002. Prediction of sediment load concentration in rivers using artificial neural network model. J. Hydraul. Eng. – ASCE 128, 588–595. doi: 10.1061/(ASCE)0733-9429(2002)128:6(588).

Nash, J.E., Sutcliffe, J.V., 1970. River flow forecasting through conceptual models. Part I: a discussion of principles. J. Hydrol. 10, 282–290.

Nogushi, S., Abduhl Rahim, N., Baharuddin, K., Makoto, T., Toshiaki, S., Kazuhito, M., 1997. Soil physical properties and preferential flow pathways in tropical rain forest, Bukit Tarek, Peninsular Malaysia. J. Forest Res. 2, 115–120.

Nortcliff, S., Thornes, J.B., 1984. Floodplain response of a small tropical stream. In: Burt, T.P., Walling, D.E. (Eds.), Catchment Experiments in Fluvial Geomorphology. Geobooks, Norwich, pp. 73–85.

O'Loughlin, C.L., Rowe, L.K., Pearce, A.J., 1978. Sediment yields from small forested catchments North Westland – Nelson, New Zealand. J. Hydrol. NZ 17, 1–15.

Peters, D.L., Buttle, J.M., Taylor, C.H., LaZerte, B.D., 1995. Runoff production in a forested, shallow soil, Canadian Shield basin. Water Resour. Res. 31, 1291–1304.

R Development Core Team, 2009. R: A Language and Environment for Statistical Computing. R Foundation for Statistical Computing, Vienna, Austria. <http://www.R-project.org>. ISBN: 3-900051-07-0

Rey, F., 2003. Influence of vegetation distribution on sediment yield in forested marly gullies. Catena 50, 549–562.

Roose, E.J., 1979. Dynamique actuelle d'un sol ferrallitique très désaturé sur sédiments argilo-sableux sous culture et sous forêt dense humide subéquatoriale du sud de la Côte d'Ivoire Adiopodoumé: 1964 à 1976. Cah. ORSTOM, sér. Pédol. 17, 259–281.

Rouse, W.C., Reading, A.J., Walsh, R.P.D., 1986. Volcanic soil properties in Dominica, West Indies. Eng. Geol. 23, 1–28.

Sayer, E.J., Tanner, E.V.J., Cheesman, A.W., 2006a. Increased litterfall changes fine root distribution in a moist tropical forest. Plant Soil 281, 5–13. doi:10.1007/s11104-005-6334-x.

Sayer, A.M., Walsh, R.P.D., Bidin, K., 2006b. Pipeflow suspended sediment dynamics and their contribution to stream sediment budgets in small rainforest catchments, Sabah, Malaysia. Forest Ecol. Manage. 224, 119–134. doi:10.1016/j.foreco.2005.12.012.

Sayer, A.M., Walsh, R.P.D., Clarke, M.A., Bidin, K., 2004. The role of pipe erosion and slopewash in sediment redistribution in small rainforest catchments, Sabah, Malaysia. In: Golosov, V., Belyaev, V., Walling, D.E. (Eds.), Sediment Transfer through the Fluvial System. IAHS Publ., vol. 288, Centre for Ecology and Hydrology, Wallingford, UK, pp. 29–36.

Schellekens, J., Scatena, F.N., Bruijnzeel, L.A., van Dijk, A.I.J.M., Groen, M.M.A., van Hogezand, R.J.P., 2004. Stormflow generation in a small rainforest catchment in the Luquillo Experimental Forest, Puerto Rico. Hydrol. Process. 18, 505–530. doi:10.1002/hyp.1335.

Schnabel, S., Maneta, M., 2005. Comparison of a neural network and a regression model to estimate suspended sediment in a semiarid basin. In: Batalla, R.J., Garcia, C. (Eds.), Geomorphological Processes and Human Impacts in River Basins. IAHS Publication No. 299, pp. 91–100.

Sidle, R.C., Tsuboyama, Y., Nogushi, S., Hosoda, I., Fujieda, M., Shimizu, T., 2000. Stormflow generation in steep forested headwaters: a linked hydrogeomorphic paradigm. Hydrol. Process. 14, 369–385.

Sidle, R.C., Ziegler, A.D., Negishi, J.N., Nik, A.R., Siew, R., Turkelboom, F., 2006. Erosion processes in steep terrain – truths, myths, and uncertainties related to forest management in Southeast Asia. Forest Ecol. Manage. 224, 199–225. doi:10.1016/j.foreco.2005.12.019.

Sinun, W., Meng, W.W., Douglas, I., Spencer, T., 1992. Throughfall, stemflow, overland flow and throughflow in the Ulu Segama rain forest, Sabah, Malaysia. Philos. Trans. Roy. Soc. B – Biol. Sci. 335, 389–395.

Smith, H.G., Dragovich, D., 2009. Interpreting sediment delivery processes using suspended sediment-discharge hysteresis patterns from nested upland catchments, south-eastern Australia. Hydrol. Process. 23, 2415–2426. doi:10.1002/hyp.7357.

Stark, N.M., Jordan, C.F., 1978. Nutrient retention by the root mat of an Amazonian rain forest. Ecology 59, 434–437.

Stickler, C.M., Nepstad, D.C., Coe, M.T., McGrath, D.G., Rodrigues, H.O., Walker, W.S., Soares-Filho, B.S., Davidson, E.A., 2009. The potential ecological costs and cobenefits of REDD: a critical review and case study from the Amazon region. Glob. Change Biol. 15, 2803–2824. doi:10.1111/j.1365-2486.2009.02109.x.

Stott, T., Leeks, G., Marks, S., Sawyer, A., 2001. Environmentally sensitive plot-scale timber harvesting: impacts on suspended sediment, bedload and bank erosion dynamics. J. Environ. Manage. 63, 3–25. doi:10.1006/jema.2001.0459.

Swank, W.T., Vose, J.M., Elliott, K.J., 2001. Long-term hydrologic and water quality responses following commercial clearcutting of mixed hardwoods on a southern Appalachian catchment. Forest Ecol. Manage. 143, 163–178.

Tromp-van Meerveld, H.J., McDonnell, J.J., 2006. Threshold relations in subsurface stormflow: 1. A 147-storm analysis of the Panola hillslope. Water Resour. Res. 42, W02410. doi:10.1029/2004WR003778.

Verbist, B., Poesen, J., van Noordwijk, M., Widianto, Suprayogo D., Agus, F., Deckers, J., 2010. Factors affecting soil loss at plot scale and sediment yield at catchment scale in a tropical volcanic agroforestry landscape. Catena 80, 34–46. doi:10.1016/j.catena.2009.08.007.

Vincent, A.G., Turner, B.L., Tanner, E.V.J., 2010. Soil organic phosphorus dynamics following perturbation of litter cycling in a tropical moist forest. Eur. J. Soil Sci. 61, 48–57. doi:10.1111/j.1365-2389.2009.01200.x.

Walling, D.E., 1984. Dissolved loads and their measurements. In: Hadley, R.F., Walling, D.E. (Eds.), Erosion and Sediment Yield: Some Methods of Measurements and Modeling. Geo Books, London, pp. 111–177.

Wieder, W.R., Cleveland, C.C., Townsend, A.R., 2009. Controls over leaf litter decomposition in wet tropical forests. Ecology 90, 3333–3341.

Wierda, A., Veen, A.W.L., Hutjes, R.W.A., 1989. Infiltration at the Tai rain forest (Ivory Coast): measurements and modelling. Hydrol. Process. 3, 371–382.

Woodring, W., 1958. Geology of Barro Colorado Island, Canal Zone, Smithsonian Miscellaneous Collections, pp. 135.

Yavitt, J.B., 2000. Nutrient dynamics of soil derived from different parent material on Barro Colorado Island, Panama. Biotropica 32, 198–207.

Ziegler, A.D., Giambelluca, T.W., Tran, L.T., Vana, T.T., Nullet, M.A., Fox, J., Vien, T.D., Pinthong, J., Maxwell, J.F., Evett, S., 2004. Hydrological consequences of landscape fragmentation in mountainous northern Vietnam: evidence of accelerated overland flow generation. J. Hydrol. 287, 124–146. doi:10.1016/j.jhydrol.2003.09.027.

Zimmermann, A., Zimmermann, B., Elsenbeer, H., 2009. Rainfall redistribution in a tropical forest: spatial and temporal patterns. Water Resour. Res. 45, W11413. doi:10.1029/2008WR007470.